JOURNAL OF THERMOPHYSICS AND HEAT TRANSFER
Vol. 16, No. 2, April–June 2002

Thermal Disturbances in Near Critical Fluids

Howard Wagner* and Yildiz Bayazitoglu†
Rice University, Houston, Texas 77005

Previous research into the piston effect used only the van der Waals equation of state for numerical simulation of the piston effect at conditions very close to the critical point. The real gas equation of state is used to compare the pressure and temperature response of oxygen and hydrogen at the critical pressure contained between two infinite parallel plates due to a thermal disturbance at one boundary. The plates were fixed with a separation distance of 2.5 mm. The bulk fluid was initialized to various temperatures ranging from 0.50 to 0.95 times the critical temperature, and then one plate would undergo a step change to 1 K above the critical temperature. The pressure rise in hydrogen after five acoustic time periods was only 17% of the pressure rise in oxygen. The temperature increase in hydrogen was only 30% of the temperature rise in oxygen. On the diffusion timescale, the pressure rise in the oxygen is an order of magnitude larger than the pressure rise in hydrogen for the same thermal penetration depth. The temperature rise in oxygen is four times greater than the temperature rise in hydrogen.

Nomenclature

C_p	=	specific heat at constant pressure
C_v	=	specific heat at constant volume
c	=	speed of sound
D_{th}	=	thermal diffusivity
k	=	thermal conductivity
L	=	characteristic length
P	=	pressure
P_c	=	critical point pressure
T	=	temperature
T_{bulk}	=	bulk fluid temperature
T_c	=	critical point temperature
T_{wall}	=	wall temperature
t_a	=	acoustic time, L/c
t_D	=	diffusion time, L^2/D_{th}
u	=	velocity
α	=	isothermal bulk modulus
β	=	volume expansivity
γ	=	ratio of specific heats
μ	=	kinematic viscosity
ν	=	dynamic viscosity
ρ	=	density

Introduction

A NEW means of heat transfer, known as the piston effect, was identified in the late 1980s by experimenters studying the specific heat of a fluid very close to the critical point. The temperature of the bulk fluid was observed to be increasing faster than could be explained by diffusion alone. The piston effect is where an expanding thermal boundary layer acts like a piston, which compresses the bulk fluid. The expansion of the thermal boundary layer also creates a pressure wave traveling at near the speed of the sound in the fluid, which transfers energy into the bulk fluid causing a temperature rise in the bulk fluid. The usual approach in estimating the time for a system to reach thermal equilibrium has been to apply the thermal diffusion equation to the system geometry with some appropriate intermediate value of the thermodynamic properties. This approach works well when the system is far away from the critical point of the fluid. Near the critical point, however, the experimentally measured time for thermal equilibrium indicated an equilibrium time much shorter than predicted by the diffusion equation. The pressure wave contributes to an energy equation source term, which results in a nearly uniform heating of the bulk fluid. The bulk fluid temperature achieves 90% of the steady-state value in less than 5% of the time predicted by diffusion alone. It was, therefore, determined that the effect of acoustic heating on the bulk fluid needs to be accounted for. Kassoy[1] conducted a theoretical investigation of the response of a confined perfect gas to a small thermal disturbance. He showed that an acoustic wave is generated in any fluid within a confined volume when the boundary temperature is suddenly changed. Boukari et al.[2] performed a numerical simulation of the thermal response of a layer of liquid initially at the critical point of the fluid. The authors considered both a sudden quenching of the boundaries of the one-dimensional container and a continuous increase in one of the boundary temperatures. When the boundary temperature was suddenly decreased from 20 mK above the critical temperature to 10 mK above the critical temperature, the bulk fluid achieved 99% of the thermal response within 5 s, significantly less time than predicted by diffusion alone. Around the same time, Zappoli et al.[3] performed a numerical analysis of carbon dioxide and saw similar results. Onuki and Ferrell[4] also obtained similar results when they used linear hydrodynamic theory to study analytically adiabatic heat transfer to a fluid near the critical point.

Behringer et al.[5] studied the thermal equilibration times for pure normal helium and mixtures of normal helium and superfluid helium. By the use of linearized hydrodynamic theory and Laplace transforms, they solved the Navier–Stokes and energy equations to determine the transient thermal response of the system under either constant pressure or constant volume conditions. They found that when the fluid temperature is greater than the critical temperature the thermal equilibration time for a fluid with a specific heat ratio γ for values $\gamma \gg 1$ in a constant volume system was four times faster than for a constant pressure system. The agreement between the constant pressure and constant volume systems becomes much better when the fluid temperature is closer to the critical temperature. They also found very little difference between the equilibration times for a pure fluid and a binary fluid. The adiabatic effect was more pronounced for larger values of the specific heat ratio.

By the use of one-dimensional hydrodynamic theory, Zappoli[6] and Djennaoui et al.[7] performed an asymptotic solution of the one-dimensional Navier–Stokes equation for a van der Waals fluid near the critical point. Their predicted thermal equilibration time agrees

Received 31 July 2001; revision received 31 October 2001; accepted for publication 1 November 2001.

*Graduate Student, Mechanical Engineering and Materials Science Department, 6100 Main Street, MS 321; hwagner@rice.edu. Associate Fellow AIAA.

†H. S. Cameron Endowed Chair Professor in Mechanical Engineering, Mechanical Engineering and Materials Science Department, 6100 Main Street, MS 321; bayaz@rice.edu. Member AIAA.

with the predictions of Onuki and Ferrell.[4] Later Zappoli et al.[8] extended their previous one-dimensional hydrodynamic equations to include two-dimensional unsteady heat transfer effects and gravity. Their efforts demonstrated that the piston effect was still present in a normal Earth gravity condition and results in fast thermal equilibration of the bulk fluid before the onset of buoyancy-driven convection. The density gradient remaining after the thermal equilibration is the driving mechanism for the onset of convection.

The research just listed used the van der Waals equation of state for numerical simulation of the piston effect at conditions very close to the critical point. In Ref. 9, the use of the van der Waals equation of state was compared to a real gas equation of state. The piston effect was investigated at bulk fluid temperatures lower than the critical temperature, representative of conditions encountered in actual cryogenic storage systems. Employing the van der Waals equation of state for numerical simulation of the piston effect results in underpredicting the magnitude of the pressure wave by 38% while overpredicting the acoustic heating by 13% compared to using a real gas equation of state. When numerically simulating the piston effect at conditions typical of cryogenic storage systems, the pressure response of the fluid was observed to be tens of kilopascals, six orders of magnitude larger than had been reported in previous research. The extent of the acoustic heating resulted in temperature increases in the bulk fluid that was measured in tens of milli-Kelvin. Previous researchers reported temperature increases in micro-Kelvin, four orders of magnitude smaller than observed by the authors. The research described in this paper uses the real gas equation of state to compare the pressure and temperature response of oxygen and hydrogen at the critical pressure contained between two infinite parallel plates due to a thermal disturbance at one boundary.

Theory

A theoretical basis for predicting the pressure sensitivity of a fluid near the critical point can be developed by examining the equations of motion and heat transfer. From the fundamental equations, the significant fluid properties can be identified, and their contribution to the fast thermal equilibration and extreme pressure sensitivity of a fluid near the critical point can be explained. The conservation equations for an unsteady one-dimensional system are given for mass, momentum, and energy, respectively, by

$$\frac{\partial \rho}{\partial t} + \frac{\partial}{\partial x}(\rho u) = 0 \tag{1}$$

$$\frac{\partial \rho u}{\partial t} + \frac{\partial \rho u^2}{\partial x} = -\frac{\partial P}{\partial x} + \frac{\partial}{\partial x}\left(\frac{4}{3}\mu \frac{\partial u}{\partial x}\right) \tag{2}$$

$$\frac{\partial}{\partial t}(\rho T) + \frac{\partial}{\partial x}\left(\rho u T - \frac{k}{C_v}\frac{\partial T}{\partial x}\right) = -\frac{T}{C_v}\left(\frac{\partial P}{\partial T}\right)_\rho \left(\frac{\partial u}{\partial x}\right) + \frac{k}{C_v^2}\left(\frac{\partial T}{\partial x}\frac{\partial C_v}{\partial x}\right) \tag{3}$$

$$\rho = f(P, T) \tag{4}$$

The boundary conditions are

$$\frac{\partial P}{\partial x} = 0 \quad \text{at} \quad x = 0, L \tag{5}$$

$$u = 0 \quad \text{at} \quad x = 0, L \tag{6}$$

$$T = T_c + 1\,\text{K} \quad \text{at} \quad x = 0 \tag{7}$$

$$T = T_{\text{bulk}} \quad \text{at} \quad x = L \tag{8}$$

The initial conditions are

$$P = P_c \tag{9}$$

$$T = T_{\text{bulk}} \tag{10}$$

$$U = 0 \tag{11}$$

The equation of state [Eq. (4)] employed in this research is the 33-term polynomial form developed by the National Institute of Standards and Technology (NIST). Readers interested in the details of the equations provided by NIST are referred to Ref. 10. For most fluids, the pressure gradient dominates the momentum equation source term because the viscosity is very small. This is valid for cryogenic fluids regardless of the proximity to the critical point. Gravity effects are not included in either the momentum or energy equations to better observe the piston effect because the relative magnitude of convective heat transfer induced by gravity would mask the effects from the acoustic heating. This form of the energy equation for a compressible fluid is a slight modification of the form given by Arpaci and Larsen.[11] The difference is that the specific heat was brought inside of the derivative for the thermal conductivity. This results in creating a source term involving the derivative of the specific heat. A dimensional analysis was performed on the entire energy equation to determine which portions of the source term are of significance. The viscous heating contribution was determined to be ten orders of magnitude smaller than the acoustic heating term and can be neglected. The kinetic heating and diffusion terms were also neglected with respect to the acoustic heating term. The only contributions to the source term result from the acoustic heating and the variable specific heat. Reflection boundary conditions are applied at both the left and right boundaries, which gives zero pressure gradient and zero velocity at each boundary. If the bulk fluid is initialized at temperatures very close to the critical temperature, then the pressure boundary condition at the right boundary must change from a reflection condition to an outflow boundary condition.[12] The very large compressibility of the fluid near the critical point results in conditions where the right pressure boundary condition needs to be treated as a rarefication boundary to model properly the fluid behavior. The conditions encountered during this research effort did not require this change in the pressure boundary condition. The right boundary is maintained at the bulk fluid temperature while the left boundary is set to 1 K above the critical temperature. The fluid is initially at rest at the critical pressure and the fluid temperature T_{bulk}.

When the energy equation (3) is examined some additional observations can be made. As the fluid approaches the critical point, C_v increases greatly, and the effect of the right-hand side can be neglected. Thus, the effect of acoustic heating is important only outside of the thermal boundary layer. On the left-hand side of the equation, the ratio of the thermal conductivity over the specific heat diverges to infinity, and the thermal gradient term dominates the time dependence of the temperature. The energy equation source term shows that heating in the bulk fluid results from the fluid motion. The pressure derivative acts as an amplification factor and is a function of the chosen equation of state.

According to the real gas equation of state, the pressure derivative is

$$\left(\frac{\partial P}{\partial T}\right)_\rho = -\alpha\beta \tag{12}$$

$$\alpha = -\rho\left(\frac{\partial P}{\partial \rho}\right)_T \tag{13}$$

$$\beta = \frac{(1/\rho)(\partial P/\partial T)_\rho}{(\partial P/\partial \rho)_T} \tag{14}$$

where α is the isothermal bulk modulus and β is the volume expansivity.

The thermal diffusivity for a constant pressure process is given by $D_{\text{th}} = k/\rho C_p$. When approaching the critical point, C_p diverges approximately twice as fast as the thermal conductivity, and, therefore, the thermal diffusivity goes to zero. As a result, extremely long thermal equilibration times are predicted, explaining the common observation of slowing thermal equilibration when approaching the critical point. This observation applies only for a constant pressure process. The thermal diffusivity for a constant volume process

is given by $D_{\text{th}} = k/\rho C_v$. In this case, the thermal conductivity diverges faster than C_v, and the thermal diffusivity goes to infinity. The thermal equilibration time for a constant volume process, therefore, approaches zero, speeding up when approaching the critical point.

Two different timescales are identified in this problem: the acoustic time and the diffusion time. The acoustic time, $t_a = L/c$, is the time required for the pressure wave to travel the length of the container. The diffusion time, $t_D = L^2/D_{\text{th}}$, is the time for a temperature change to be transmitted the length of the container by pure diffusion. The acoustic time is much smaller than the diffusion time, demonstrating the higher relative rate of heat transferred by the piston effect compared to diffusion alone. Kassoy[1] showed that the strength of the acoustic wave is dependent on the magnitude of the temperature change and how rapidly the fluid properties vary with temperature. Because the fluid properties show the greatest sensitivity at the critical point, this suggests that the acoustic waves will be strongest when near the critical point of the fluid.

Analysis

Oxygen and hydrogen were selected for this study to examine fluid behavior near the critical point for a poor heat transfer fluid and a good heat transfer fluid, respectively. The thermophysical properties involved in the momentum and energy equations are the density, thermal conductivity, constant volume specific heat, isothermal compressibility (the inverse of the isothermal bulk modulus), and the volume expansivity. Their contribution to the piston effect is described subsequently. The most important properties for the piston effect were determined to be the thermal conductivity, the volume expansivity, and the isothermal compressibility. The thermal conductivity and the volume expansivity determine the thickness of the thermal boundary layer. The isothermal compressibility determines the pressure response of the bulk fluid to the change in volume of the thermal boundary layer.

Thermodynamic Properties

The thermodynamic properties utilized in this research effort were calculated using a computer program originally created by NIST[10] in 1980 for NASA Johnson Space Center. The program reproduces the values from the published NIST tables for 15 cryogenic fluids. The program accurately reproduces the divergence of the fluid properties at the critical point. The output from the program was compared to the published tables from NIST with very close correlation, often within 1% of the tabulated values except near the critical point, where the maximum error is estimated to be about 10%. Readers interested in the details of the equations provided by NIST are referred to Ref. 10.

Density

The variation of density with temperature and pressure for both fluids near the critical point is shown in Fig. 1. The critical pressure P_c and the critical temperature T_c for oxygen are 5043 kPa and 154.58 K, respectively, and for hydrogen are 1315 kPa and 33.19 K, respectively. To compare more directly the two fluids, the reduced temperature is defined as the fluid temperature divided by the critical temperature for that fluid. There is a slight increase in density as the pressure is increased. The density of both fluids decreases as the temperature is increased, with a steep gradient at the critical temperature. The density of oxygen is about 16 times larger than that of hydrogen. From the continuity equation, higher velocities are expected in hydrogen than in oxygen.

Viscosity

The variation of viscosity with temperature and pressure for both fluids near the critical point is shown in Fig. 2. The viscosity of both fluids decreases as the temperature is increased. A steep gradient in viscosity occurs at the critical temperature. There is a slight increase in viscosity as the pressure is increased. The viscosity of oxygen is about eight times that of hydrogen. The NIST program[10] did not include the viscosity of hydrogen, and so a curve fit was performed on the published National Bureau of Standards (NBS) tables[13] to generate the needed equations. The details of the curve fit results are discussed by Wagner et al.[14]

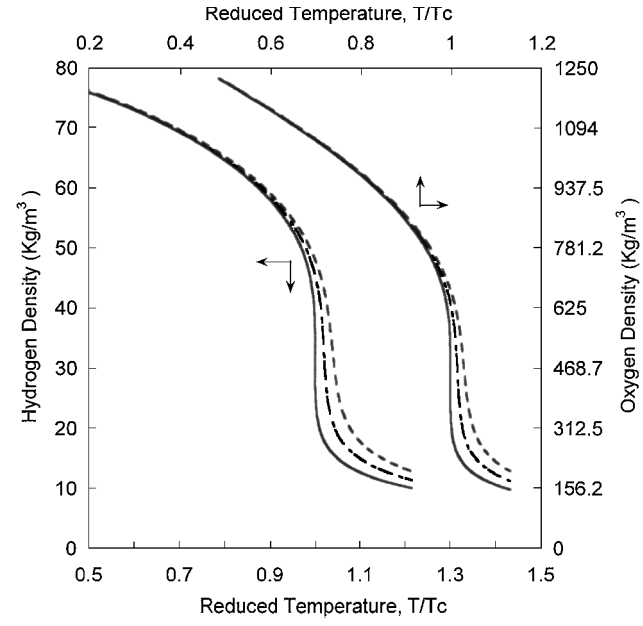

Fig. 1 Variation of density with temperature and pressure: solid line is data from NIST equation of state at critical pressure, short dashes are data from NIST equation of state at 1.1 times critical pressure, and long dashes are data from NIST equation of state at 1.2 times critical pressure.

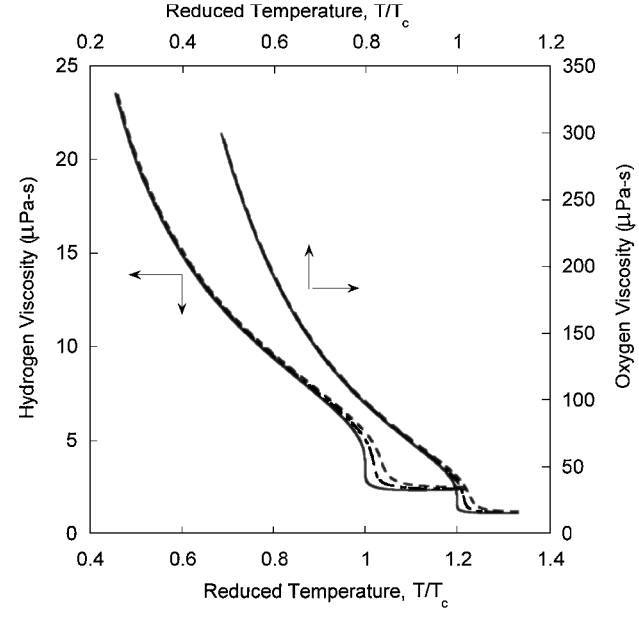

Fig. 2 Variation of viscosity with temperature and pressure: solid line is data from NIST equation of state at critical pressure, short dashes are data from NIST equation of state at 1.1 times critical pressure, and long dashes are data from NIST equation of state at 1.2 times critical pressure.

Specific Heat

The variation of the specific heats at constant volume with temperature and pressure for both fluids near the critical point is shown in Fig. 3. The specific heat, and therefore the heat transfer capability, of oxygen decreases as the temperature is increased, whereas that of hydrogen increases. Both fluids exhibit a sharp increase in the specific heat at the critical point. This behavior supports the observation that most fluids become extremely good heat transport fluids near the critical point. The specific heat of hydrogen is approximately seven times greater than that of oxygen.

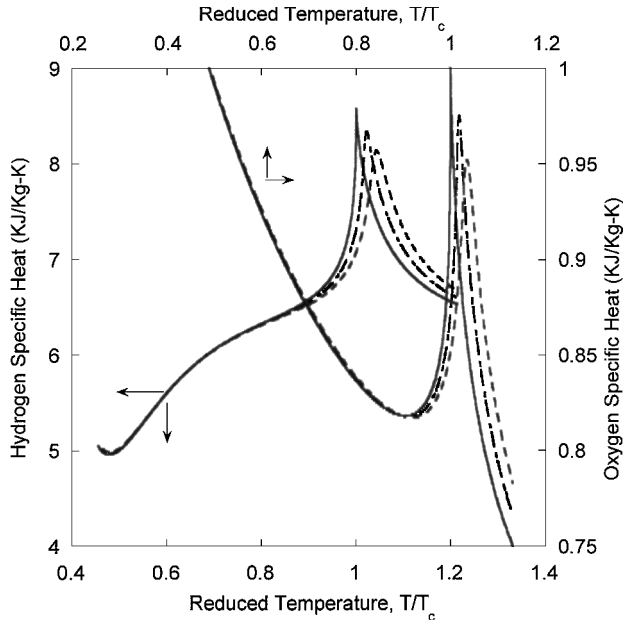

Fig. 3 Variation of specific heat with temperature and pressure: solid line is data from NIST equation of state at critical pressure, short dashes are data from NIST equation of state at 1.1 times critical pressure, and long dashes are data from NIST equation of state at 1.2 times critical pressure.

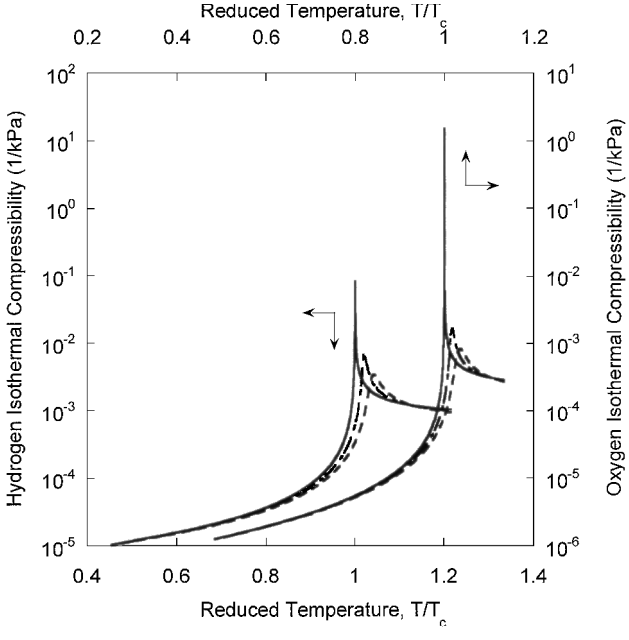

Fig. 4 Variation of isothermal compressibility with temperature and pressure, multiplied by −1 for plotting purposes: solid line is data from NIST equation of state at critical pressure, short dashes are data from NIST equation of state at 1.1 times critical pressure, and long dashes are data from NIST equation of state at 1.2 times critical pressure.

Isothermal Compressibility

The variation of the isothermal compressibility with temperature and pressure for both fluids near the critical point is shown in Fig. 4. The isothermal compressibility is the inverse of the isothermal bulk modulus and is shown multiplied by −1 to simplify the plot. Both fluids show an extreme sensitivity to pressure changes near the critical point. The magnitude of the divergence at the critical point decreases as the pressure increases. For a small pressure change, both fluids would undergo a large volume change when near the critical point. The inverse also holds true: For a large volume change, the pressure would change only a small amount when near the critical

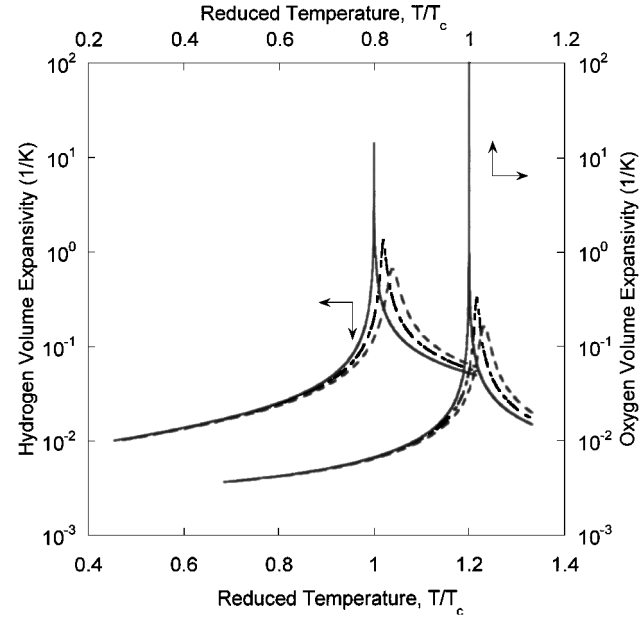

Fig. 5 Variation of volume expansivity with temperature and pressure: solid line is data from NIST equation of state at critical pressure, short dashes are data from NIST equation of state at 1.1 times critical pressure, and long dashes are data from NIST equation of state at 1.2 times critical pressure.

point. If the fluid is much colder than the critical temperature, it will respond as an incompressible fluid. Therefore, the compressibility effects will be isolated to the thermal penetration region. The isothermal compressibility of hydrogen is about an order of magnitude larger than that of oxygen, such that the same change in volume of the bulk fluid produces for hydrogen $\frac{1}{10}$th the pressure change of oxygen.

Volume Expansivity

The variation of the volume expansivity with temperature and pressure for both fluids near the critical point is shown in Fig. 5. As the pressure increases, the magnitude of the divergence at the critical point decreases. Both fluids show an extreme sensitivity to temperature changes near the critical point, where a large volume change results from a small temperature change in the fluid. The volume expansivity determines the thickness of the thermal penetration region, which may experience a sudden increase or decrease resulting from a temperature disturbance at the boundary. A temperature increase at the boundary will result in an expansion of the thermal penetration region and an increase in the pressure. A temperature decrease at the boundary or forced fluid mixing between the thermal penetration region and the bulk fluid will result in shrinkage of the thermal penetration region and a pressure decrease in the bulk fluid. This sensitivity in the volume expansivity is very significant when near the critical point, but if the fluid temperature in the thermal penetration region is only a few degrees below the critical temperature, then the fluid will exhibit normal volume expansivity. Any fluid mixing would then result in small changes in both the thermal penetration region thickness and pressure. The volume expansivity of hydrogen is twice that of oxygen. For a given change in temperature at the boundary, the thermal penetration depth of hydrogen would change twice as much as it would for oxygen.

Thermal Conductivity

The variation of thermal conductivities with temperature and pressure of both fluids near the critical point is shown in Fig. 6. The NIST program[10] did not include the thermal conductivity of hydrogen, and so a curve fit was performed on the published NBS tables[13] to generate the needed equations. The details of the curve fit results are discussed by Wagner et al.[14] The thermal conductivity of hydrogen is an order of magnitude larger than that of oxygen.

Table 1 Speed of sound of oxygen and acoustic times used for the numerical simulations

Temperature, K	Reduced temperature T/T_c	Speed of sound, m/s	Acoustic time μ, s	Thermal diffusivity, cm^2/s	Diffusion time, s
154.581	1.00	154.15	16.22	$5.799 \times 10^{+3}$	1.08×10^{-5}
146.85	0.95	388.19	6.44	3.366×10^{-4}	185.68
139.12	0.90	492.08	5.08	4.548×10^{-4}	137.42
131.39	0.85	576.40	4.34	5.385×10^{-4}	116.06
123.66	0.80	650.98	3.84	6.057×10^{-4}	103.19
115.94	0.75	719.60	3.47	6.627×10^{-4}	94.31
108.21	0.70	784.49	3.19	7.126×10^{-4}	87.71
100.48	0.65	846.82	2.95	7.566×10^{-4}	82.61
92.75	0.60	907.54	2.76	7.953×10^{-4}	78.59
85.02	0.55	967.37	2.58	8.292×10^{-4}	75.37
77.29	0.50	1026.72	2.44	8.585×10^{-4}	72.80

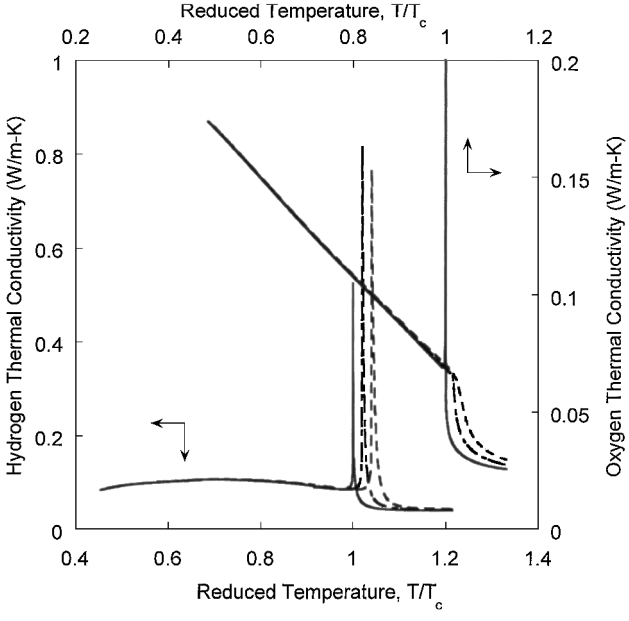

Fig. 6 Variation of thermal conductivity with temperature and pressure: solid line is data from NIST equation of state at critical pressure, short dashes are data from NIST equation of state at 1.1 times critical pressure, and long dashes are data from NIST equation of state at 1.2 times critical pressure.

The magnitude of the divergence at the critical point decreases as the pressure increases. The thermal conductivity of oxygen decreases as the fluid temperature is increased, whereas the thermal conductivity of hydrogen shows little variation for temperatures less than the critical temperature. The decreasing thermal conductivity will result in an increasing thickness of the thermal penetration region. The thermal conductivity of hydrogen shows a much larger divergence at the critical point than does oxygen. As the hydrogen temperature approaches the critical point, the thermal conductivity will rapidly increase, resulting in a thinner thermal penetration depth. This means there will be a much smaller volume change in the bulk fluid when the thermal penetration region thickness is decreased. Therefore, it can be expected to see a large pressure change in oxygen, but only a small pressure change in hydrogen, when the thermal penetration depth is decreased.

Analytical Model

A solution algorithm was desired that could handle the extreme compressibility expected near the critical point. The SIMPLE algorithm developed by Patankar[15] was selected because it avoids the problems that could be encountered with most solution algorithms that employ the speed of sound as a scaling factor to normalize the fluid velocities. The fluid velocities encountered in this research are very small, and scaling with the speed of sound would increase the stiffness of the solution matrix. Because the algorithm treats only the time step explicitly and all other parameters implicitly, it allows for a wide range of time step and grid sizes while providing a stable solution.

Problem Description

The pressure sensitivity near the critical point was investigated by performing a number of one-dimensional numerical analyses using the properties of oxygen and hydrogen. The pressure increase and the bulk fluid temperature increase in hydrogen were compared to the respective increases in oxygen. The pressure and temperature increases in oxygen contained between two infinite parallel plates were evaluated at the critical pressure. The plates were fixed with a separation distance of 2.5 mm. The bulk fluid temperature was initialized to various values ranging from 0.50 to 0.95 times the critical temperature, and then one plate would undergo a step change to 1 K above the critical temperature. The simulations employed a time step of half the acoustic time period $t_a/2$ and ran for a total of five acoustic time periods $5t_a$, which was sufficient for the pressure to return to a nearly uniform condition after the temperature disturbance at the boundary. The acoustic time period was adjusted for each run based on the speed of sound in the bulk fluid. The values used in the numerical analyses of oxygen are shown in Table 1. A grid sensitivity study was performed to determine the number of nodes needed to result in an acceptable accuracy. The peak pressure showed a 5% change when the number of nodes was increased from 5,000 to 10,000, but showed a change of less than 1% when increased further to 15,000. Thus, it was determined that 10,000 nodes would provide an acceptable accuracy. The same analyses were repeated, but this time using hydrogen as the fluid. The values used in the numerical analyses of hydrogen are shown in Table 2. For the hydrogen simulations, a grid of 10,000 nodes was also used.

Acoustic Time Period

The following results were all evaluated using a reduced temperature of the bulk fluid of 0.75 where the reduced temperature is the fluid temperature divided by the critical temperature. Results at other bulk fluid temperatures demonstrate similar trends. The pressure and velocity profiles after half an acoustic time period for oxygen and hydrogen are shown in Fig. 7. The peak pressure for oxygen is about five times that of hydrogen, as predicted in the discussion on the isothermal compressibility and the thermal conductivity. The discussion on density of the two fluids suggested higher velocities in hydrogen than in oxygen, and the peak velocity in hydrogen is almost twice that of oxygen.

After five acoustic time periods, the pressure rise and temperature rise in the bulk fluid were nearly uniform. The pressure rise in oxygen was 57 kPa, whereas hydrogen experienced only 17% of that value, 10 kPa. The ratio of the isothermal compressibilities predicted that the pressure rise in oxygen would be an order of magnitude larger than in hydrogen, assuming both bulk fluids experience the same volume change. The temperature rise in the

Table 2 Speed of sound of hydrogen and acoustic times used for the numerical simulations

Temperature, K	Reduced temperature T/T_c	Speed of sound, m/s	Acoustic time μ, s	Thermal diffusivity, cm^2/s	Diffusion time, s
32.938	1.00	379.05	6.60	$12.67 \times 10^{+4}$	4.93×10^{-7}
31.29	0.95	660.97	3.78	6.720×10^{-4}	93.01
29.64	0.90	785.97	3.18	9.153×10^{-4}	68.28
28.00	0.85	879.08	2.84	10.870×10^{-4}	57.50
26.35	0.80	955.42	2.62	12.261×10^{-4}	50.97
24.70	0.75	1020.19	2.45	13.452×10^{-4}	46.46
23.06	0.70	1076.41	2.32	14.504×10^{-4}	43.09
21.41	0.65	1127.28	2.22	15.464×10^{-4}	40.42
19.76	0.60	1174.83	2.13	16.323×10^{-4}	38.29
18.12	0.55	1221.47	2.05	16.992×10^{-4}	36.78
16.47	0.50	1270.41	1.97	17.110×10^{-4}	36.53

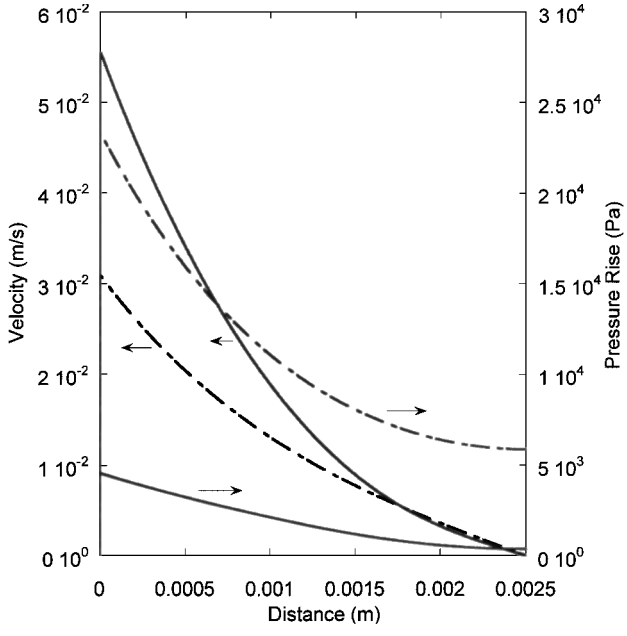

Fig. 7 Velocity and pressure profiles after half the acoustic time period: solid lines are for hydrogen and dashed lines for oxygen.

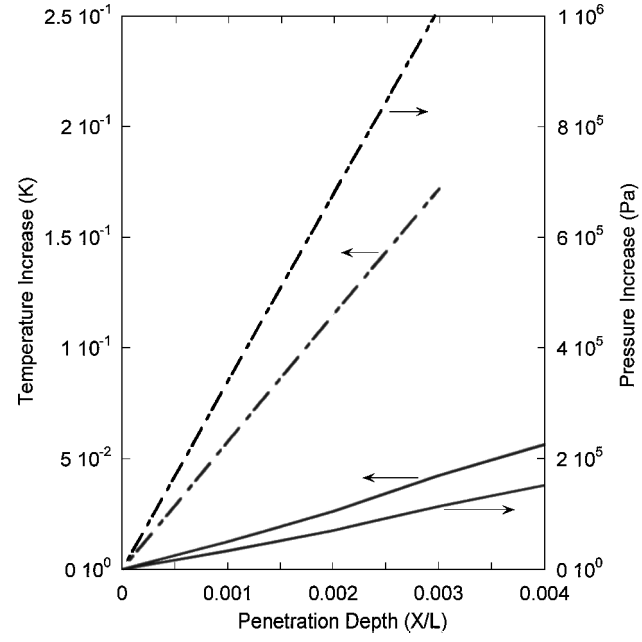

Fig. 9 Temperature and pressure increase vs thermal penetration depth at a bulk fluid reduced temperature of 0.55: solid lines are for hydrogen and dashed lines for oxygen.

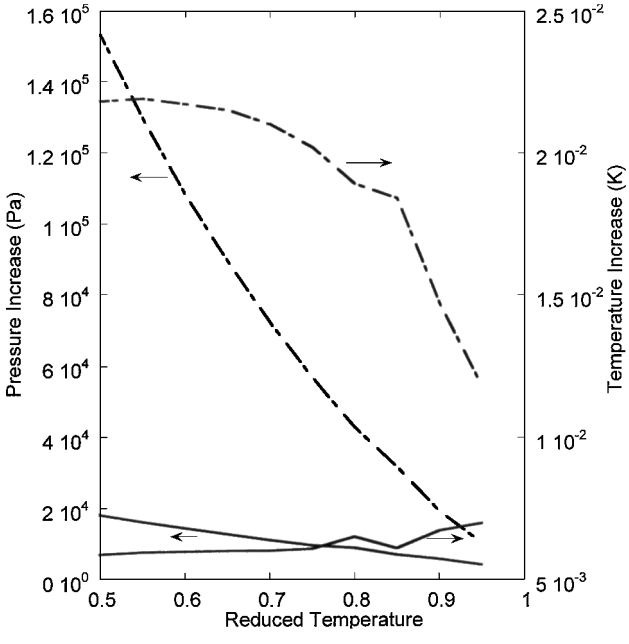

Fig. 8 Pressure and temperature increase after five acoustic time periods: solid lines are for hydrogen and dashed lines for oxygen.

bulk fluid in oxygen was 20 mK, whereas the temperature rise in hydrogen was 6 mK, 30% of that of oxygen.

The pressure and temperature increases in both fluids after five acoustic time periods are shown in Fig. 8 as a function of the reduced fluid temperature. As the bulk fluid temperature approaches the critical temperature, the compressibility of the bulk fluid increases significantly due to the divergence of the isothermal compressibility at the critical point. This means a very large volume change is required to create any significant pressure change. As a result, the pressure increase goes to zero as the reduced temperature approaches one. The pressure rise in oxygen is an order of magnitude larger than in hydrogen, corresponding to the order of magnitude difference in the isothermal compressibilities of the two fluids. The bulk fluid temperature rise in the liquid oxygen decreases as the oxygen temperature is increased. The temperature rise in the liquid hydrogen shows a slight increase as the hydrogen temperature is increased. This trend is similar to the trends in the thermal conductivity of the two fluids shown in Fig. 6.

Diffusion Time Period

The computer simulations were allowed to continue for hundreds of time steps to determine the pressure and temperature response of the bulk fluid on the diffusion timescale. The pressure and temperature increases in oxygen are compared to the respective increases in hydrogen for various thermal penetration depths in Fig. 9. The

results shown are for a representative value of the reduced temperature of 0.55. Similar trends occur at the other bulk fluid temperatures. Both fluids demonstrate a linear pressure rise vs the penetration depth. When the bulk fluid temperature is near the critical temperature, the response begins to deviate from this linear response. As the thermal penetration depth is doubled, the pressure rise is doubled. The pressure rise in the oxygen is an order of magnitude larger than the pressure rise in hydrogen for the same thermal penetration depth. This is in agreement with the discussion on the isothermal compressibilities of the two fluids. The temperature rise in both fluids also demonstrates a linear response to the thermal penetration depth. When the bulk fluid temperature is near the critical temperature, the response starts to deviate from this linear response. As the thermal penetration depth is doubled, the temperature rise is doubled. The temperature rise in oxygen is four times greater than the temperature rise in hydrogen.

Space Shuttle Observations

The order of magnitude difference in the pressure response of oxygen and hydrogen is in agreement with observations of the supercritical cryogen tanks on the space shuttle. Pressure decays of up to 2000 kPa are common in the supercritical liquid oxygen tanks. The liquid oxygen tanks will be operating around the 5516 kPa storage pressure when fluid mixing due to a thruster firing would result in the pressure dropping 500–2000 kPa in the tank. Conversely, no noticeable pressure decays have been observed in the supercritical liquid hydrogen tanks.

Conclusions

The research described used the real gas equation of state to compare the pressure and temperature response of oxygen and hydrogen to a thermal disturbance at the boundary. The pressure and temperature response was investigated on both the acoustic timescale and the diffusion timescale. The pressure rise in hydrogen after five acoustic time periods was only 17% of the pressure rise in oxygen. The temperature increase in hydrogen was only 30% of the temperature rise in oxygen. The computer simulations were allowed to continue for hundreds of time steps to determine the pressure and temperature response of the bulk fluid on the diffusion timescale. Both fluids demonstrate a linear pressure and temperature rise vs the penetration depth. The pressure rise in oxygen is an order of magnitude larger than the pressure rise in hydrogen for the same thermal penetration depth. The temperature rise in oxygen is four times greater than the temperature rise in hydrogen.

References

[1] Kassoy, D. R., "The Response of a Confined Gas to a Thermal Disturbance. I: Slow Transients," *SIAM Journal on Applied Mathematics*, Vol. 36, No. 3, 1979, pp. 624–634.

[2] Boukari, H., Shaumeyer, J. N., Briggs, M. E., and Gammon, R. W., "Critical Speeding Up in Pure Fluids," *Physical Review A*, Vol. 41, No. 4, 1990, pp. 2260–2263.

[3] Zappoli, B., Bailly, D., Garrabos, Y., Le Neindre, B., Guenoun, P., and Beysens, D., "Anomalous Heat Transport by the Piston Effect in Supercritical Fluids Under Zero Gravity," *Physical Review A*, Vol. 41, No. 4, 1990, pp. 2264–2267.

[4] Onuki, A., and Ferrell, R., "Adiabatic Heating Effect Near the Gas–Liquid Critical Point," *Physica*, Vol. A 164, 1990, pp. 245–264.

[5] Behringer, R. P., Onuki, A., and Meyer, H., "Thermal Equilibration of Fluids Near the Liquid–Vapor Critical Point: ^{3}He and ^{3}He–^{4}He Mixtures," *Journal of Low Temperature Physics*, Vol. 81, No. 1, 1990, pp. 71–102.

[6] Zappoli, B., "The Response of a Nearly Supercritical Pure Fluid to a Thermal Disturbance," *Physics of Fluids A (Fluid Dynamics)*, Vol. 4, No. 5, 1992, pp. 1040–1048.

[7] Djennaoui, N., Heraudeau, F., Guenoun, P., Beysens, D., and Zappoli, B., "Thermal Transport in a Pure Fluid Near the Critical Point," *41st Congress of the International Astronautical Federation*, Pergamon, Elmsford, NY, 1990, pp. 189–193; also *Acta Astronautica*, Vol. 29, No. 3, 1993, pp. 189–193.

[8] Zappoli, B., Amiroudine, S., Cales, P., and Ouazzani, J., "Numerical Solutions of Thermoacoustic and Buoyancy-Driven Transport in a Near Critical Fluid," *Materials and Fluids Under Low Gravity; Proceedings of the 9th European Symposium on Gravity-Dependent Phenomena in Physical Sciences*, Lecture Notes in Physics, Vol. 464, Springer-Verlag, Berlin, 1996, pp. 27–40.

[9] Wagner, H., Hos, P., and Bayazitoglu, Y., "Variable Property Piston Effect," *Journal of Thermophysics and Heat Transfer*, Vol. 15, No. 4, 2001, pp. 497–503.

[10] McCarty, R. D., "Interactive Fortran IV Computer Programs for the Thermodynamic and Transport Properties of Selected Cryogens (Fluids Pack)," National Bureau of Standards TN 1025, U.S. Dept. of Commerce, Washington, DC, Oct. 1980.

[11] Arpaci, V. S., and Larsen, P. S., *Convection Heat Transfer*, Prentice–Hall, Englewood Cliffs, NJ, 1984, p. 49.

[12] Zappoli, B., Carles, P., Amiroudine, S., and Ouazzani, J., "Inversion of Acoustic Waves Reflection Rules in the Near Critical Pure Fluid," *Physics of Fluids*, Vol. 7, No. 9, 1995, pp. 2283–2287.

[13] McCarty, R. D., Hord, J., and Roder, H. M., "Selected Properties of Hydrogen," National Bureau of Standards, U.S. Dept. of Commerce, Washington, DC, 1981.

[14] Wagner, H., Tunc, G., and Bayazitoglu, Y., "A Model for Hydrogen Thermal Conductivity and Viscosity Including the Critical Point," *Thermal Science and Engineering*, Vol. 8, No. 5, 2000.

[15] Patankar, S. V., *Numerical Heat Transfer and Fluid Flow*, Hemisphere, Washington, DC, 1980.